Hygroscopicity issues in powder and grain technology

J. Torres-Serra
Técnicas Mecánicas Ilerdenses, S.L., Lleida, Spain
E. Romero
Universitat Politècnica de Catalunya · BarcelonaTech, Barcelona, Spain
A. Rodríguez-Ferran
Universitat Politècnica de Catalunya · BarcelonaTech, Barcelona, Spain

ABSTRACT: The effect of hygroscopicity on flowability of powders and bulk solids with applications in the packaging industry is experimentally and numerically investigated. Firstly, four granular materials are tested at different water contents to study the impact of relative humidity on some hydro-mechanical properties, namely the hydraulic diffusivity on wetting, as well as the shear strength and compressibility properties of the materials. Next, a capillary model covering a wider water content range –compared to the previous tests– is applied to discrete element simulations of a granular column collapse set-up. These simulations give further insight into important aspects of grain hygroscopicity in packaging and other industrial applications (such as the kinematics of flow and flowability issues), which are outside the scope of conventional experimental testing.

1 INTRODUCTION

Relative humidity affects the amount of stored water in powders and bulk solids, which has important consequences on the efficiency of bulk handling equipment used in the packaging industry. Flowability of granular materials is crucial to performance assessment of conveying techniques, as discussed by Leturia et al. (2014). The role of hygroscopicity on the constitutive behaviour of bulk solids is very important and has been recently addressed by Juarez-Enriquez et al. (2017). Relative humidity is known to influence phenomena such as slip-stick or caking, as indicated by Pozo et al. (2008), and Hartmann and Palzer (2011).

The authors have developed a new prototype, see Torres-Serra et al. (2017a), which allows performing column collapse tests on materials at different water contents, thus observing the impact of moisture on their flowability and the properties of the kinematics of flow. The prototype consists of a quasi-two-dimensional set-up with a reservoir containing a granular pile, which is instantaneously released onto a horizontal channel with vertical glass walls where runout takes place. A preliminary characterisation programme to better define sample preparation at different water contents for the column collapse tests has been followed and is presented in this paper. Several bulk solids are studied focusing on water absorption properties, as well as on compressibility and shear strength properties at different moisture contents.

The authors have also performed numerical simulations, see Torres-Serra et al. (2017b), to anticipate the impact of absorbed water on run-out and on different mobility parameters in granular column collapse tests. Discrete element simulations using a liquid bridge model have been implemented and selected results at different liquid contents corresponding to the pendular regime are presented at the end of the paper.

2 EXPERIMENTAL STUDY

2.1 *Water absorption in an environmental chamber*

Water vapour absorption diffusivity of granular materials allows predicting the storage time in an environmental chamber to reach equilibrium at imposed ranges of relative humidity, *RH*. Water vapour sorption phenomenon is studied using a desiccator at room temperature 20°C with pure water placed at the bottom of the desiccator to apply the largest water content changes.

Four samples of height around 20 mm and initial $RH = 60\%$ are kept in the environmental chamber, comprising: a) adhesive mortar, b) natural zeolite, and c) wheat flour ('flour' and 'flour 2'). The initial properties of the samples are summarised in Table 1, including the median particle size, D_{50}, which is obtained from the particle size distribution by sieve analysis using ASTM series sieves, as shown in Figure 1. A laser particle size analyser is used with the mortar sample to determine the fraction finer than sieve No. 200 (75 μm), where water is mainly stored. Some shifting towards a coarser grading associated

with the laser technique compared to the sieve analysis can be observed.

Table 1. Initial properties of tested samples.

	Gravimetric water content[a], w (%)	Bulk density, ρ_b (kg/m^3)	Median particle size[b], D_{50} (μm)
Mortar	2.1	1188	148 (348[c])
Zeolite	5.8	647	165
Flour	20	467	109
Flour 2	13	489	–

[a] Water content values at RH = 60% (ψ = 69 MPa)
[b] Sieve analysis [c] Laser particle size analyser

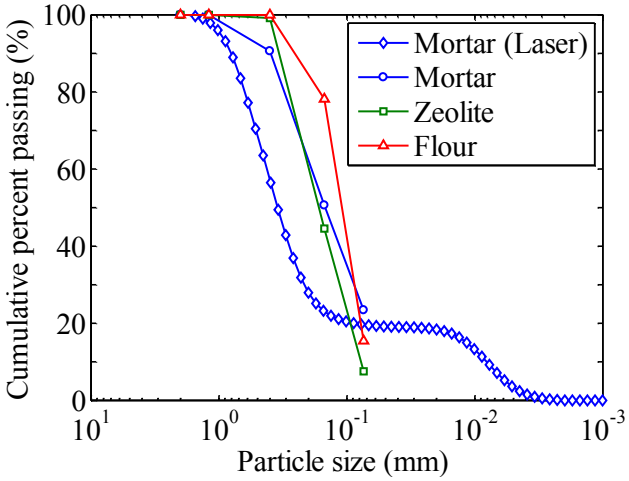

Figure 1. Particle size distribution curves for mortar, zeolite and flour samples.

Mass changes during wetting are regularly determined along 14 days, as shown in Figure 2. Total suction, ψ, of the samples at the end of this period is measured using a dew point psychrometer (WP4-T Dewpoint PotentiaMeter, Decagon Devices Inc, US). Time evolution of absorbed water is estimated by a constant diffusivity model, see for instance Kunze and Kirkham (1962):

$$\frac{Q(t)}{Q_0} = 1 - \frac{8}{\pi^2}\sum_{m=0}^{\infty}\frac{1}{(2m+1)^2}\exp\left(-(2m+1)^2\pi^2\frac{D_w t}{4L^2}\right) \quad (1)$$

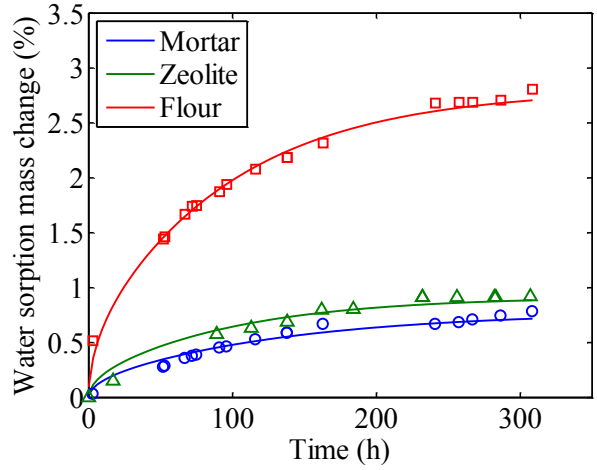

Figure 2. Water vapour sorption for mortar, zeolite and flour samples.

where $Q(t)$ is the amount of absorbed water at time t, Q_0 is the total amount of absorbed water in the suction step, D_w is capillary diffusivity, and L is the sample drainage height. Data in Figure 2 is fitted to Equation 1 and capillary diffusivity determined.

Equilibrated conditions and diffusivity results for mortar, zeolite and flour samples are summarised in Table 2. As observed in the table, despite imposing a relatively high RH, the materials are only able to reach RH values between 65 and 75%. This is associated with skin effects due to the saturation of the sample surface in contact with the humid atmosphere, which slows down the migration of vapour into the bulk material.

Table 2. Typical equilibrium environmental chamber conditions of mortar and flour samples.

	Mortar	Zeolite	Flour
Gravimetric water content, w (%)	2.8	6.7	23
Total suction, ψ (MPa)	58	–	40
Relative humidity, RH (%)	65	–	75
Capillary diffusivity, $D_w \cdot 10^{-10}$ (m^2/s)	3.3	4.5	4.5

2.2 *Oedometer cell*

Compressibility of bulk solids has an effect on packing configuration of particle systems, as reported by Santomaso et al. (2003) Therefore, the pouring procedure by which granular columns are formed in the reservoir of the flowability prototype presented by Torres-Serra et al. (2017a) has an impact on the initial packing condition of the material. The testing procedure considers gravity-driven flows at different initial moisture contents (controlled by RH) and packing states: poured random packing due to free fall, loose packing obtained from poured packing by an imposed airflow, and dense packing resulting from deaeration of initially poured packing.

The effect of water content of the samples on their compressibility is studied by performing step loading tests under oedometer conditions. Samples at initial and equilibrated water contents are tested. Test results for zeolite and flour 2 samples are shown in Figure 3. Maximum compressibility index, C_c^*, is defined by:

$$C_c^* = \frac{\Delta\varepsilon_a}{\Delta\log\sigma} \quad (2)$$

where $\Delta\varepsilon_a$ is the change in axial strain, and $\Delta\log\sigma$ is the increment of log-scale axial stress.

No clear effect of water content on compressibility is observed, since similar compressibility indexes are obtained in both zeolite and flour 2 samples at slightly different water contents. This can be explained in terms of the relatively small changes in water content undergone by the materials in the environmental chamber due to skin effects. Further tests are required at contrasting water contents to better define the effect of moisture on material compressibility.

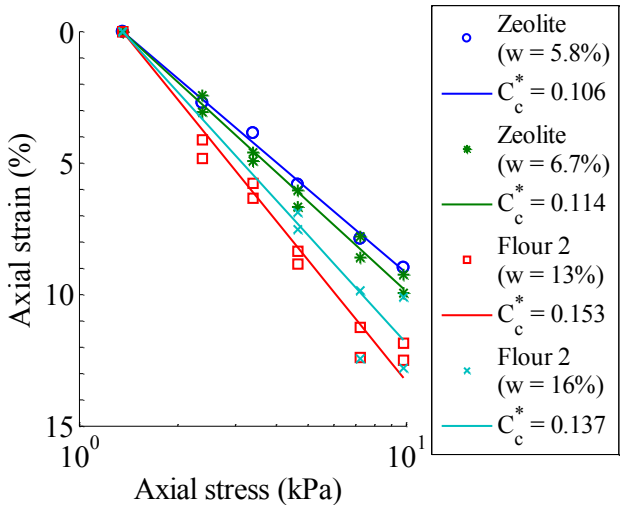

Figure 3. Step loading tests for zeolite and flour samples at slightly different water contents.

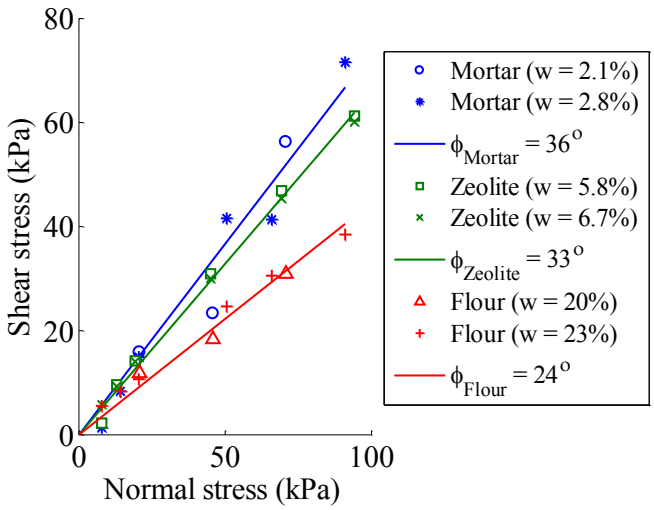

Figure 5. Shear strength and angle of friction at residual state for mortar, zeolite and flour samples at slightly different water contents.

2.3 *Residual shear strength in ring shear apparatus*

Usually, flowability has been assessed by measuring shear strength properties at large displacements of granular materials, see Schwedes (2003). Samples of three materials at slightly different water contents are tested using a ring shear apparatus to capture the shear strength properties at residual state. The evolution of shear stress with displacement for the different samples is shown in Figure 4.

Stick-slip behaviour, spontaneous jerking motion on sliding, is known to be affected by *RH* and is linked to the formation of water menisci, as described by Cain et al. (2001). This behaviour is mainly observed for flour at 23% water content in Figure 4, where larger fluctuations in the shear stress are detected along shearing.

Similar shear stresses at large displacements and given normal stress are observed despite the different water contents. Romero et al. (2014) observed clear differences in the residual shear strength of clayey soils at different water contents associated with aggregate stiffness and size. The small variations in residual shear strength of the current study can be explained by the relatively small changes in water content that the materials undergo, between 0.8% and 2.8%. This is better appreciated when plotting the residual shear strength results at different normal stresses, which are shown in Figure 5. The friction angle under residual conditions, ϕ, is defined as:

$$\phi = \tan^{-1}\frac{\tau_{res}}{\sigma} \tag{3}$$

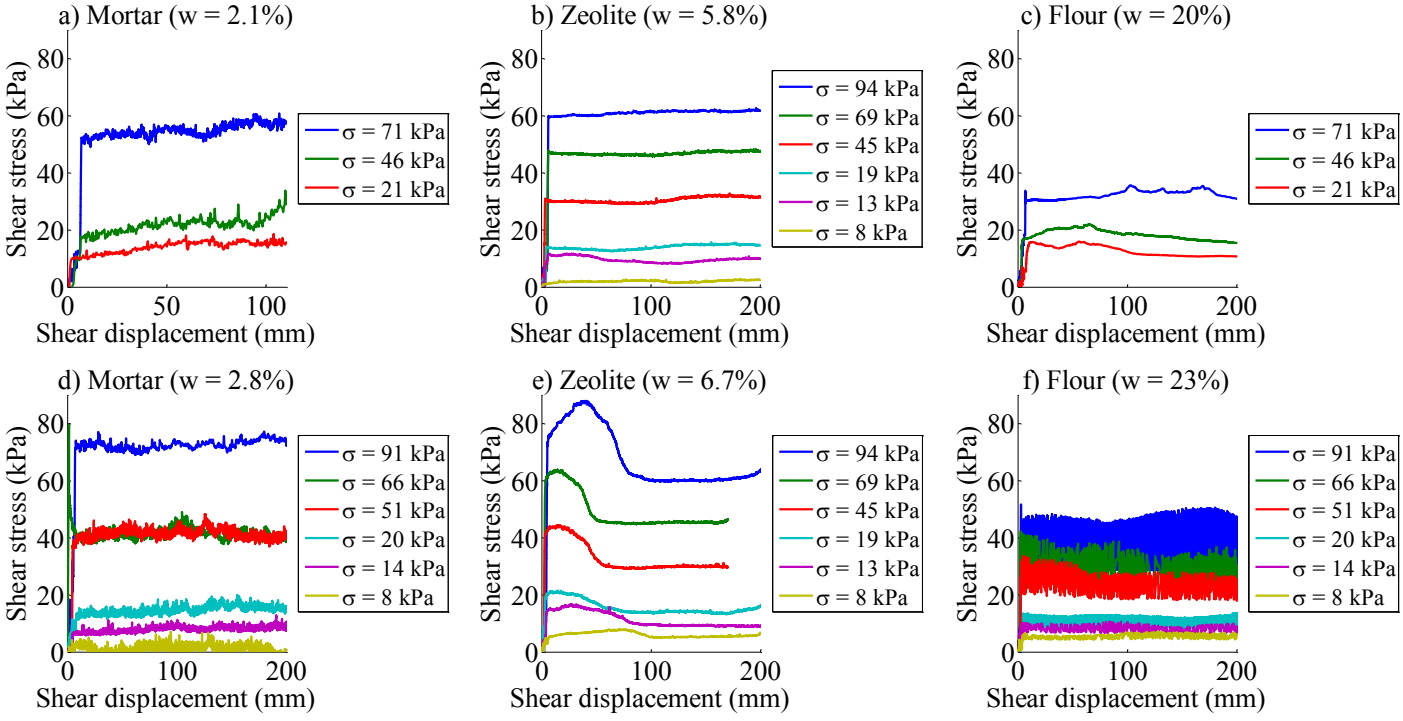

Figure 4. Shear stress versus horizontal shear displacement for mortar, zeolite and flour samples with different water contents.

where τ_{res} is the mean residual shear strength and σ the normal stress. Results presented in Figure 5 show higher friction angles at residual state for mortar and zeolite (between ϕ = 35° and 36°) than for flour (ϕ = 24°).

3 NUMERICAL SIMULATIONS

3.1 *Set-up of granular column collapse test*

A quasi-two-dimensional simulation of a granular column collapse set-up is studied. The domain consists of a prismatic horizontal channel of length 2150 mm, height 350 mm and width 150 mm, along which run-out takes place. An auxiliary vertical wall is initially placed at a distance of 150 mm, which forms a cuboid-shaped reservoir where the granular columns are generated, as shown in Figure 6. Wet granular piles are allowed settling in the reservoir under gravity, until stationary initial packing conditions are reached. After that, particles are instantaneously released onto the channel by removing the boundary condition of null horizontal displacement along the channel direction.

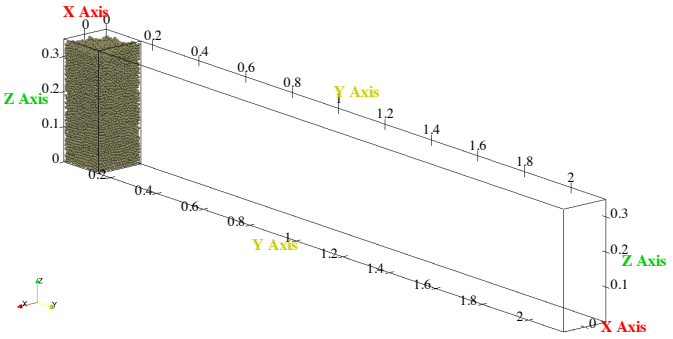

Figure 6. Simulation set-up of the granular column collapse channel. Dimensions in (m).

Table 3. Inter-particle contact parameters of granular column collapse simulations.

Parameters	Value
Stiffness	
Normal, k_n (N/m)	$1.0 \cdot 10^4$
Tangential, k_t (N/m)	$0.2 \times k_n$
Rolling, k_r (N/m)	$0.1 \times k_n$
Torsional, k_o (N/m)	$0.1 \times k_n$
Dissipation	
Normal, γ_n (N·s/m)	0.3
Tangential, γ_t (N·s/m)	$0.2 \times \gamma_n$
Rolling, γ_r (N·s/m)	$0.05 \times \gamma_n$
Torsional, γ_o (N·s/m)	$0.05 \times \gamma_n$
Friction coefficient	
Tangential, μ_t (N/m)	0.5
Rolling, μ_r (N/m)	$0.1 \times \mu_t$
Torsional, μ_o (N/m)	$0.1 \times \mu_t$

A particle system with 15500 spherical particles of radius 4 mm (coarser particles than the median size of tested materials) and particle density ρ_p = 950 kg/m^3 is simulated. These larger particles can be considered as aggregates of finer particles. The linear spring–dashpot contact model presented by Luding (2008) is used, with mechanical properties shown in Table 3.

3.2 *Liquid bridge model*

The effect of hygroscopicity on the flow behaviour of the granular slope is investigated by modelling capillary effects corresponding to the pendular state, as described by Iveson et al. (2002). Liquid is assumed to be adsorbed in the form of liquid films and capillary liquid bridges between particles. Liquid bridges are commonly modelled using the approximation given by Willett et al. (2000), according to which the contribution of capillary force, f_c, is combined with the linear normal force, f_n, as shown by Roy et al. (2015):

$$f_n = \begin{cases} 0 & \delta_n \le -d \\ -f_c & -d < \delta_n \le 0 \\ k_n \delta_n + \gamma_n v_n - f_c & \delta_n > 0 \end{cases} \quad (4)$$

where δ_n is interparticle overlap, v_n is the normal component of relative velocity, and $d > 0$ is the rupture distance acting only during particle separation. Liquid bridge formation mechanism is assumed to neglect water adsorption effects during particle approach: liquid bridges are created when particles come into contact ($\delta_n > 0$).

Capillary model parameters are shown in Table 4. Surface tension is increased by one order of magnitude with respect to water surface tension (0.073 N/m at room temperature), to allow observing the effect of liquid bridges more clearly for coarse-grained particle systems.

Table 4. Liquid bridge model parameters of granular column collapse simulations.

Parameters	Value
Surface tension, σ (N/m)	0.725
Contact angle, θ (°)	30
Maximum liquid bridge volume (m^3)	$2.0 \cdot 10^{-8}$
Distribution coefficient	0.8

Gravimetric liquid content is imposed so that the total liquid volume, Q, is homogeneously distributed among the particles at start, which is computed by:

$$Q = w \frac{\rho_p}{\rho_w} V_p \quad (5)$$

where V_p is the total volume of the spherical particles system.

3.3 *Simulation results*

Discrete particle simulations are carried out using the open-source code MercuryDPM, see Weinhart et al. (2017). The initial column aspect ratio is 2.1, defined as column height versus side width. Simulations range from w = 0% to 25% gravimetric liquid content, thus lying within the range of pendular state occurrence, according to Mitarai and Nori (2006).

Figure 7 shows lateral views of the granular pile during collapse. At time 1 s after the onset of flow, collapse has taken place and the final deposit is formed. The effect of liquid bridges on run-out distance is observed to increase with the total liquid content, by slowing down collapse (for w = 1%) and even stopping flow out of the reservoir (for w = 11% and 25%). As expected, water contents in the range of pendular regime reduce flowability of granular materials. This behaviour can be seen as the contribution of liquid bridges on caking of powders and bulk solids, as described by Zafar et al. (2017).

4 CONCLUSIONS

Results of the experimental study show that only small water content changes are obtained using the environmental chamber procedure, despite samples being kept at elevated relative humidity conditions. In the desiccator, a saturated skin effect is developed by which water is stored in small pores on the surface layer of the sample exposed to saturated relative humidity conditions. This prevents water vapour permeation into the bulk material. Therefore, the effects of moisture content on compressibility or on residual shear strength are not observed as clearly as expected. Further tests with improved wetting technologies will be carried out to better cover a wider water content range, as found in industrial applications.

Despite the low-stress levels usually involved in industrial applications, conventional soil testing equipment adapted for higher stresses has proven to give reasonable results for the tested granular materials.

Finally, numerical techniques have allowed studying a wider water content range within the pendular regime compared to the experimental tests. Results of the numerical simulations show that the formation of particle aggregates motivated by the hygroscopic behaviour of the materials can be reproduced by applying a liquid bridge model to discrete element simulations. To do so, coarse particle packings are used and liquid surface tension is scaled accordingly. More realistic model parameters will be used when extending our research to larger systems of finer-grained particles.

5 ACKNOWLEDGEMENTS

The authors would like to acknowledge the financial support provided by Project 2014 DI 075, *Optimization of dosing systems for bulk solids using experimental and numerical techniques*, funded by the Industrial Doctorates Plan of the Government of Catalonia.

REFERENCES

Cain, R., Page, N., & Biggs, S. 2001. Microscopic and Macroscopic Aspects of Stick-Slip Motion in Granular Shear. *Physical Review E* 64(1):16413.

Hartmann, M., & Palzer, S. 2011. Caking of Amorphous Powders — Material Aspects, Modelling and Applications. *Powder Technology* 206(1–2):112–21.

Iveson, S. M., Beathe, J. A., & Page, N. W. 2002. The Dynamic Strength of Partially Saturated Powder Compacts: The Effect

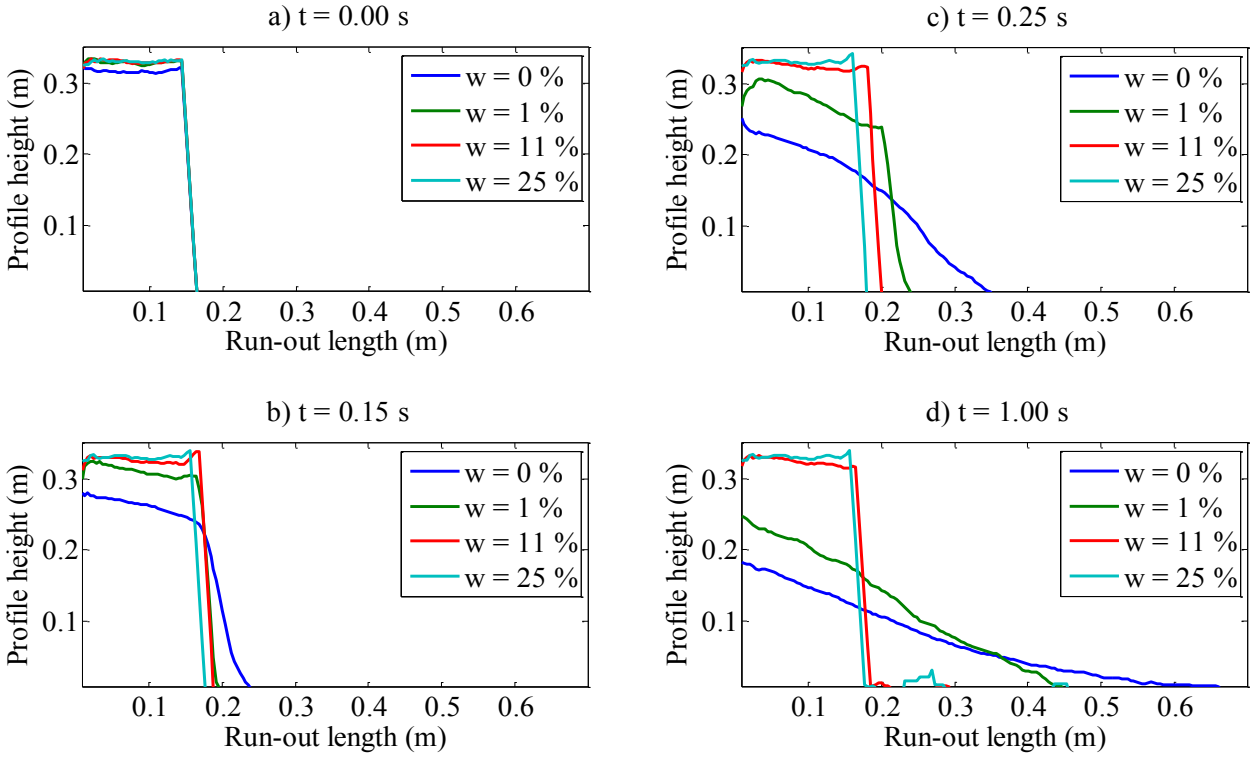

Figure 7. X-averaged lateral profiles of granular column collapse after the onset of flow.

of Liquid Properties. *Powder Technology* 127(2):149–61.
Juarez-Enriquez, E., Olivas, G. I., Zamudio-Flores, P. B., Ortega-Rivas, E., Perez-Vega, S., & Sepulveda, D. R. 2017. Effect of Water Content on the Flowability of Hygroscopic Powders. *Journal of Food Engineering* 205:12–17.
Kunze, R. J., & Kirkham, D. 1962. Simplified Accounting for Membrane Impedance in Capillary Conductivity Determinations1. *Soil Science Society of America Journal* 26(5):421.
Leturia, M., Benali, M., Lagarde, S., Ronga, I., & Saleh, K. 2014. Characterization of Flow Properties of Cohesive Powders: A Comparative Study of Traditional and New Testing Methods. *Powder Technology* 253:406–23.
Luding, S. 2008. Introduction to Discrete Element Methods. Basics of Contact Force Models and How to Perform the Micro-Macro Transition to Continuum Theory. *European Journal of Environmental and Civil Engineering* 12(7–8):785–826.
Mitarai, N., & Nori, F. 2006. Wet Granular Materials. *Advances in Physics* 55(1–2):1–45.
Pozo, O., Soulestin, B., & Olivi-Tran, N. 2008. Stick Slip Motion in Grain Grain Friction in a Humid Atmosphere. *Multidiscipline Modeling in Materials and Structures* 4(4):393–405.
Romero, E., Vaunat, J., & Merchán, V. 2014. Suction Effects on the Residual Shear Strength of Clays. *Journal of Geo-Engineering Sciences* 2:17–37.
Roy, S., Luding, S., & Weinhart, T. 2015. Towards Hydrodynamic Simulations of Wet Particle Systems. *Procedia Engineering* 102(53):1531–38.
Santomaso, A., Lazzaro, P., & Canu, P. 2003. Powder Flowability and Density Ratios: The Impact of Granules Packing. *Chemical Engineering Science* 58(13):2857–74.
Schwedes, J. 2003. Review on Testers for Measuring Flow Properties of Bulk Solids. *Granular Matter* 5:1–43.
Torres-Serra, J., Romero, E., Rodríguez-Ferran, A., Caba, J., Arderiu, X., Padullés, J.-M., & González, J. 2017a. Flowability of Granular Materials with Industrial Applications - An Experimental Approach. *EPJ Web of Conferences* 140:3068.
Torres-Serra, J., Tunuguntla, D. R., Denissen, I. F. C., Rodríguez-Ferran, A., & Romero, E. 2017b. Discrete Element Modelling of Granular Column Collapse Tests with Industrial Applications. In *V International Conference on Particle-Based Methods – Fundamentals and Applications (PARTICLES 2017)*, 530–38.
Weinhart, T., Tunuguntla, D. R., Schrojenstein Lantman, M. P. van, Denissen, I. F., Windows-Yule, C. R., Polman, H., Tsang, J. M. F., Jin, B., Orefice, L., Vaart, K. van der, et al. 2017. MercuryDPM: Fast, Flexible Particle Simulations in Complex Geometries - Part B. Applications. In *V International Conference on Particle-Based Methods – Fundamentals and Applications (PARTICLES 2017)*, 123–34.
Willett, C. D., Adams, M. J., Johnson, S. A., & Seville, J. P. K. 2000. Capillary Bridges between Two Spherical Bodies. *Langmuir* 16(24):9396–9405.
Zafar, U., Vivacqua, V., Calvert, G., Ghadiri, M., & Cleaver, J. A. S. 2017. A Review of Bulk Powder Caking. *Powder Technology* 313:389–401.